# Truncated disc versus extremely broad iron line in XTE J1650-500

Done, Chris; Gierliński, Marek

*Published in:*
Monthly Notices of the Royal Astronomical Society

*DOI:*
10.1111/j.1365-2966.2005.09968.x

*Publication date:*
2006

*Licence:*
No Licence / Unknown

*Document Version*
Publisher's PDF, also known as Version of record

Mon. Not. R. Astron. Soc. **367,** 659–668 (2006) doi:10.1111/j.1365-2966.2005.09968.x

# Truncated disc versus extremely broad iron line in XTE J1650−500

Chris Done[1] and Marek Gierliński[1,2]★

[1]*Department of Physics, University of Durham, South Road, Durham DH1 3LE*
[2]*Obserwatorium Astronomiczne Uniwersytetu Jagiellońskiego, 30-244 Kraków, Orla 171, Poland*

Accepted 2005 December 7. Received 2005 December 7; in original form 2005 October 20

**ABSTRACT**

There is growing evidence from both spectral and timing properties that there is a truncated inner accretion disc in low mass accretion rate Galactic black hole systems. The detection of *extremely* smeared relativistic iron lines in some of these systems is the *only* current piece of evidence which conflicts with this geometrical interpretation of the low/hard state. Here, we show that the line width in the *BeppoSAX* data of a bright low/hard state of the transient black hole XTE J1650−500 is indeed consistent with extreme relativistic effects. However, the relativistic smearing can be *significantly* reduced if there is also resonance iron K line *absorption* from an outflowing disc wind. The iron line smearing is then completely compatible with a truncated disc, so it gives no information on the black hole spin.

**Key words:** accretion, accretion discs – black hole physics – X-rays: binaries – X-rays: individual: XTE J1650−500.

## 1 INTRODUCTION

The existence of a minimum stable orbit for material around a black hole is a key prediction of general relativity in the strong-field limit. For Schwarzschild black holes this is at $R_{\rm ms} = 6R_g$ (where $R_g = GM/c^2$), while for maximally rotating Kerr black holes (spin parameter $a = 0.998$) this reduces to $1.23R_g$. Bright accretion flows give a way to observationally test such ideas as well as to directly estimate the spin of the black hole. Optically thick material in Keplerian orbits should emit a quasi-thermal spectrum with maximum-temperature emission from the largest-luminosity/smallest-area regions, i.e. set by the last stable orbit (Shakura & Sunyaev 1973). As these models are thermal, there is a clear prediction that their maximum temperature, $T_{\rm max}$, should increase with total disc luminosity as $L_{\rm disc} \propto T_{\rm max}^4$, if the emission is from a constant area, i.e. if there is a constant inner disc radius. Strong observational support for this comes from the Galactic black hole (GBH) binary systems. These can show disc-dominated spectra (often termed the high/soft state) where $L_{\rm disc} \propto T_{\rm max}^4$ over large changes in luminosity (Ebisawa et al. 1993; Kubota, Makishima & Ebisawa 2001; Kubota & Makishima 2004). The fixed radius inferred from the proportionality constant of this relation is consistent with a Keplerian disc (stress-free inner boundary condition) in a low-to-moderate spin space–time ($a \lesssim 0.8$) for all GBH for which this experiment can be performed (Gierliński & Done 2004; Davis, Done & Blaes in preparation; Li et al. 2005; Shafee et al. 2005). This ties in with the spins expected from models of stellar collapse. These predict a maximum birth spin of $a \sim 0.8$ from the combination of slow rotation of the pre-supernovae core and angular momentum losses through gravitational wave radiation during collapse (e.g. Gammie, Shapiro & McKinney 2004), and there is not enough mass transfer in the binary evolution to cause appreciable spin-up from accretion (King & Kolb 1999).

However, there is growing evidence that the accretion disc inner radius can also be *larger* than $R_{\rm ms}$, due to the inner disc evaporating into hot, geometrically thick accretion flow. These models were developed in response to observations of GBH at low-luminosity (generally termed the low/hard state), where the expected accretion disc emission is much weaker and at lower temperature than that predicted by an optically thick disc extending down to the last stable orbit (e.g. Esin et al. 2001; Frontera et al. 2001). Instead, the X-ray spectra peak at ∼100 keV (see e.g. the review by Zdziarski & Gierliński 2004), requiring that the continuum is formed in hot, optically thin plasma, which is not strongly cooled by Compton scattering of seed photons (e.g. Zdziarski & Gierliński 2004). These cooling limits are very difficult (Barrio, Done & Nayakshin 2003; though not impossible, e.g. Beloborodov 1999) to reconcile with a cool disc extending down to the minimum stable orbit. Other observational advantages of truncated disc configuration is that it can provide a geometric explanation for the major X-ray spectral state transitions seen in GBH by a physical change in the accretion flow structure. At low luminosities the inner cool disc is replaced by a hot accretion flow. The transition radius between the two phases is far from the hole, few photons from the disc illuminate the hot flow and the spectrum is hard. As the transition radius moves inwards the disc penetrates further into the hot flow, so more seed photons cool the flow and its spectrum softens until the disc extends down to the last stable orbit (Esin, McClintock & Narayan 1997). This changing transition radius also gives a changing size scale to associate with the changing characteristic frequencies seen in the variability power spectra (see e.g. the review by Done 2001).

★E-mail: Marek.Gierlinski@durham.ac.uk

Theoretically, such hot inner flows are generically produced by a range of analytic approximations to the accretion flow equations. In these, the protons are heated by gravity, while the electrons gain energy only through Coulomb collisions and cool predominantly via Compton scattering (Shapiro, Lightman & Eardley 1976), advection (Narayan & Yi 1995), outflows (Blandford & Begelman 1999), convection (Abramowicz & Igumenshchev 2001) or jets (Falcke, Körding & Markoff 2004). Numerical simulations of the accretion flow at low densities, including the self-consistently generated magnetic dynamo viscosity (Balbus & Hawley 1991), appear to show some form of inner hot flow, though its properties are more complex than any of the approximate analytic solutions above (Hawley & Balbus 2002).

Another argument for the truncated disc comes from the quasi-periodic oscillations (QPOs) observed in the power-density spectra of black hole binaries. During the transition from the low/hard to the high/soft spectral state their frequency typically increases (e.g. Cui et al. 1999; Rossi et al. 2004) indicating a decreasing size scale in the accretion flow. If the QPO frequency is directly related to the transition radius between the cold disc and the hot inner flow (Stella & Vietri 1998; Titarchuk, Osherovich & Kuznetsov 1999; Psaltis & Norman 2000) then its behaviour is consistent with a decreasing truncation radius as the source approaches the soft state.

Clearly, the point at which the cool disc truncates is of great importance to our understanding of the nature of the accretion flow, and hence whether we can use observations of compact objects to test strong gravity. Fortunately, there is an independent constraint on this from the shape of the fluorescent iron line produced by X-ray illumination of the cool disc. Special and general relativistic effects are both important as the disc material is in very high-velocity (Keplerian) orbits in a strong gravitational field. All these effects get stronger as the disc extends closer to the black hole, so the width of the line gives a measure of the inner edge of the cool fluorescing material (Fabian et al. 1989, 2000). Thus for the accretion flow model above in which there is a variable truncation radius between a disc and inner hot flow, the line width should be correlated with spectral hardness. Hard spectra (generally seen at low $L/L_{\rm Edd}$) should have narrow lines, softer spectra should have broader lines. There are indications that this correlation is seen both in active galactic nuclei (AGN) (Lubiński & Zdziarski 2001) and in GBH (Życki, Done & Smith 1998; Churazov, Gilfanov & Revnivtsev 2000; Ibragimov et al. 2005).

However, some of the more recent results from the line shape seen in the GBH do not fit easily into this picture. There are reported lines *in the low/hard state* (i.e. hard X-ray spectra, with QPO frequencies which are not at their maximum values) which are so broad as to require a disc around a maximally spinning black hole, illuminated by highly centrally concentrated radiation field, perhaps implying direct tapping of the spin energy of the black hole or at least substantial continuous stress across the last stable orbit (Miller et al. 2002, 2004a; Miniutti, Fabian & Miller 2004). Plainly, this would rule out the inner hot-flow model if there is no alternative explanation for the line width. The clearest example of this discrepancy is the *BeppoSAX* data of the bright low/hard state of XTE J1650−500. The line width in this spectrum is also in conflict with the moderate spin derived from the luminosity–temperature relation obtained when this object shows disc-dominated spectra (Gierliński & Done 2004). Thus, the extent of the disc inferred from the iron line width in XTE J1650−500 seems at odds with the broad-band spectral shape, the QPOs and the disc continuum emission.

Here, we re-examine the *BeppoSAX* data on XTE J1650−500 and show that while these data are indeed consistent with an extreme relativistic line, they can be fit equally well (or better) using a model of a 'normal' relativistic line (i.e. from a truncated disc with standard gravitational energy release), together with blueshifted highly ionized narrow absorption features (predominantly resonance lines of He- and H-like iron). These absorption features distort the blue edge of the line, especially where the reflection spectrum is ionized and/or viewed at high inclination. If the presence of such material is confirmed then this removes the *only* observational evidence against a truncated-disc interpretation of the low/hard state in GBH.

## 2 THE DATA

We extract the XTE J1650−500 *BeppoSAX* archival data taken in 2001 September 11 for both the medium-energy concentrator spectrometer (MECS) and phoswich detector system (PDS) instruments, using the standard (1997 September) background, auxiliary response (MECS) and redistribution files (MECS and PDS). We use the same energy ranges as Miniutti et al. (2004), i.e. 2.5–10 keV (MECS) and 13–200 keV (PDS), with 2 per cent systematic errors added in quadrature to the PDS data. We checked the publicly available Crab PDS data and obtain reduced $\chi^2/\nu = 0.9$ for a single power law of energy index 1.13, showing that this prescription is an adequate description of the response uncertainties.

We also extract the *RXTE* proportional counter array (PCA) and high-energy X-ray timing experiment (HEXTE) spectra from the entire outburst. We calculate the X-ray colours and estimate the bolometric luminosity following the method of Done & Gierliński (2003). We used the distance of 4 kpc (Tomsick et al. 2003) and mass of 7.3 $M_\odot$ (Orosz et al. 2004) for the luminosity estimate. We also extracted the power-density spectra from PCA observations in the 1/128- to 64-Hz frequency band and fitted them by a multiple Lorentzian model.

We use XSPEC version 11.3.1 (Arnaud 1996) for spectral fitting. The error of each model parameter is given for a 90 per cent confidence interval. We fix the absorption column at $N_H = 5 \times 10^{21}$ cm$^{-2}$ in all fits (Miller et al. 2002; Miniutti et al. 2004).

## 3 TIMING AND SPECTRAL EVOLUTION DURING THE OUTBURST

Fig. 1 shows the estimated bolometric luminosity, the frequency of the strong low-frequency QPO and X-ray colours obtained from the *RXTE*. The vertical line marks the time of the *BeppoSAX* observation analysed in this paper. The QPO frequency during the *BeppoSAX* observation is plainly not the maximum seen from this source. Any association of the QPO with the inner radius of the cool disc clearly requires that the disc does *not* extend down to the last stable orbit, but truncates *above* this point. The X-ray colours show that the *BeppoSAX* data were taken while the source is still smoothly softening, in a position which is associated with the softest low/hard states. Given that the spectrum softens further *after* the *BeppoSAX* observation, models of the broad-band spectra with a moving inner disc predict that the disc truncates *above* the last stable orbit. Thus, both the QPOs and broad-band spectral shape indicate that the innermost parts of a cool disc are not present. This is in conflict with the extreme iron line smearing *in these same data* which requires that the disc extends down to the last stable orbit of a high-spin black hole.

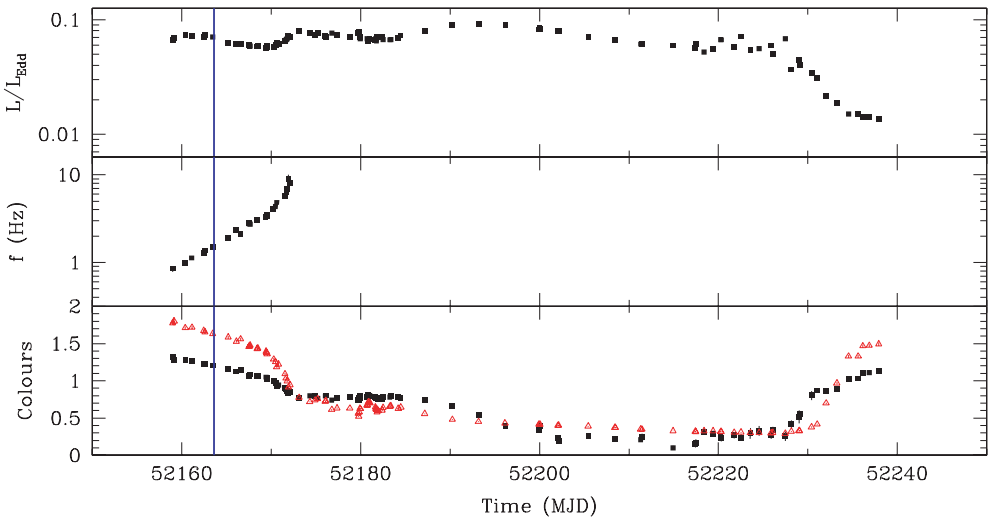


**Figure 1.** The top panel shows the evolution of the total, absorption-corrected, bolometric luminosity (in units of Eddington luminosity) for all the *RXTE* pointed observations of the outburst of XTE J1650−500. The total flux is derived from fitting the PCA and HEXTE data with a model of an accretion disc plus its Comptonized emission (together with a broad line and smeared edge to mimic reflection). The middle panel shows the low-frequency QPO derived from fitting the broad-band power spectra with multiple Lorentzian components, while the bottom panel shows the soft (triangles, red in colour) and hard (black squares) X-ray colours. Both QPO and colours are still evolving smoothly at the point where the *BeppoSAX* data were taken (vertical line). In the context of a truncated disc model for the low/hard state, this implies that the disc has not yet reached the last stable orbit.

## 4 MECS 2–10 keV DATA: 45° INCLINATION

### 4.1 Simple models

With the MECS data we can reproduce the extreme relativistic broadening of Miniutti et al. (2004). We use their phenomenological model of a smeared edge and iron line with extreme Kerr space–time distortions (the LAOR model in XSPEC) on a continuum consisting of a disc spectrum and power law. This gives an adequate fit ($\chi^2 = 70.9/65$) to the data, and the parameters of the strong iron line (equivalent width of $190^{+30}_{-20}$ eV) do indeed point to a very small inner disc radius of $r_{\rm in} \equiv R_{\rm in}/R_g = 2.20^{+0.06}_{-0.16}$ with extreme central concentration of the illumination, $\propto r^{-q}$ where $q = 4.3^{+0.4}_{-0.3}$. A similarly extreme line is seen using the same model in the *XMM–Newton* data taken a few days after the *BeppoSAX* observation (Miller et al. 2002).

The XSPEC LAOR code is written for the specific case of calculating the relativistic effects on a line which can be approximated as an initial delta function. This is identical to the transfer function, so relativistic effects on an arbitrary initial spectrum can be calculated by simply convolving the initial spectrum with this transfer function. We recoded the LAOR model into a convolution model (hereafter called CONLINE) in XSPEC and use this to smear a full reflected spectrum (the PEXRIV model in XSPEC with additional narrow Gaussian line) to replace the phenomenological smeared edge/line features in the previous fit. Convolution means that the spectrum outside of the observed energy band can be important so we always extend the energy range used by XSPEC to 0.2–50 keV.

We follow Miller et al. (2002) and Miniutti et al. (2004) and fix the inclination angle to 45° and assume solar abundances. We constrain the radial emissivity index to be between 3 and 5 as suggested by these previous fits. This gives $\chi^2 = 75.7/65$, i.e. slightly worse than the phenomenological approximation for reflected continuum emission. The best-fitting model is reflection dominated, with $\Omega/2\pi = \infty$, i.e. for a model in which the intrinsic continuum is hidden from view. However, this is poorly constrained, with the error range allowing $\Omega/2\pi > 0.7$. By contrast the line parameters are fairly well constrained, with equivalent width of $120 \pm 25$ eV, and inner disc radius of $r_{\rm in} = 2.2^{+0.18}_{-0.12}$ and $q = 3.7^{+0.3}_{-0.3}$. Thus the line parameters do change with the addition of a reflected continuum, most significantly in reducing the equivalent width, although the smearing is also affected, with the illumination being not quite so centrally concentrated. Detailed results on the line equivalent width (and to a lesser extent the shape) derived without including a reflected continuum should be treated with caution. None the less, the small disc inner radius is very similar to that in the phenomenological fits; there is a very broad feature in the data between 4 and 7 keV as shown in Fig. 2(a).

### 4.2 Complex reflection

The reflected component from the PEXRIV fits in the previous section is strongly ionized. This means that the intrinsic iron line emission from the disc is *not* narrow. It should instead be strongly Comptonized, and this Comptonization should also affect the edge in the reflected continuum (Ross, Fabian & Young 1999). The neglect of Compton scattering below 12 keV in PEXRIV means that this code has an edge which is artificially deep and sharp for a highly ionized disc. We replace the PEXRIV-reflected continuum and narrow Gaussian line with reflected spectra of D. Ballantyne from a constant-density ionized disc (hereafter CDID; Ballantyne, Iwasawa & Fabian 2001a, based on Ross & Fabian 1993) which are publicly available as XSPEC table models. These calculate the reflected spectrum from an X-ray-illuminated slab of constant density, including Compton upscattering and downscattering below 12 keV, with self-consistent iron (and other elements) line calculation for solar abundance material. These give $\chi^2 = 93.7/67$ for a highly smeared, ionized slab, somewhat worse than the (unphysical) fits above, but with two free parameters less as the line energy and width are now calculated self-consistently with the reflected continuum. The reflection emission is highly

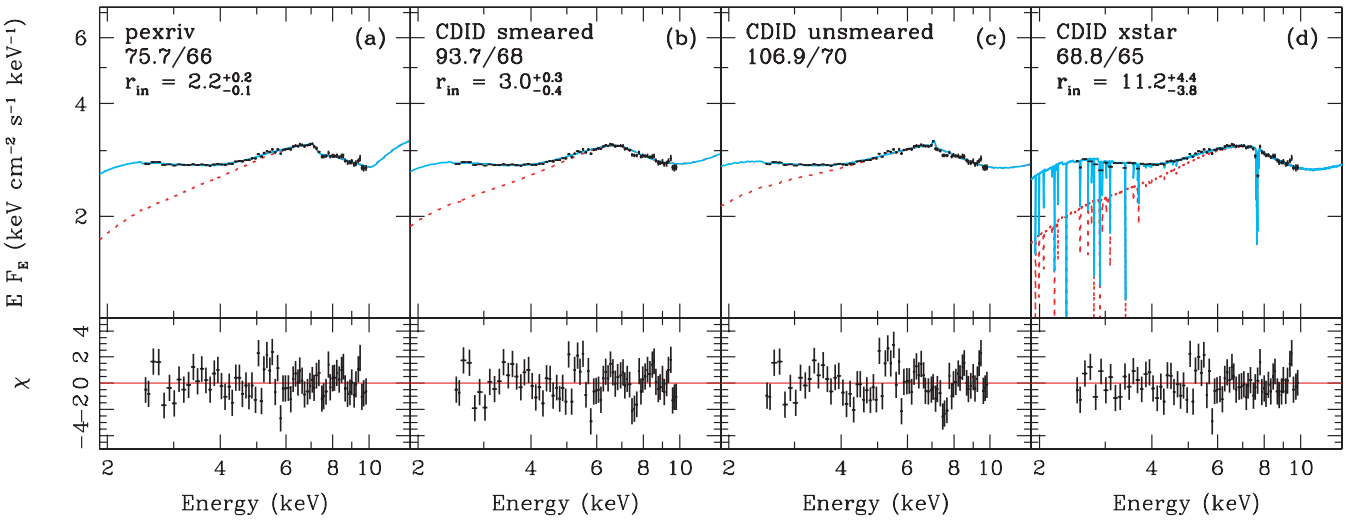


**Figure 2.** MECS data fit to solar abundance reflection assuming an inclination of 45°. The (red in colour) dotted curve corresponds to the reflection, while the solid (cyan in colour) curve shows the sum of the reflection and the disc emission which is out of scale in these figures. Panel (a) shows the best fit using PEXRIV-based reflection model, in which the reflector is highly ionized, and is extremely relativistically smeared. These relativistic effects strongly distort the intrinsic reflected spectrum. Panel (b) shows the very different reflected emission produced by CDID models, where the line and edge are intrinsically broad due to Comptonization. The best-fitting reflected spectrum is highly ionized, and extremely relativistically smeared. Panel (c) shows the same reflection model as in (b) but with *no* relativistic effects at all applied, so this fit is not dependent on inclination. The disc is again highly ionized, so the line is intrinsically broad and this intrinsic shape is a fairly good match to the data. This fit is only $\Delta\chi^2 = 13$ worse than the best fit (with the loss of two degrees of freedom). Panel (d) shows the fit including ionized *absorption* from outflowing material. The inferred relativistic smearing reduces dramatically, so this fit is relatively independent of inclination.

ionized, $\lg(\xi/\mathrm{erg\,cm\,s^{-1}}) = 3.79^{+0.03}_{-0.08}$, and again the spectrum is consistent with pure reflected continuum, although the errors are wide and only restrict $\Omega/2\pi > 0.6$.

The best fit again picks out extreme relativistic smearing, with $q = 5^{+0}_{-1.2}$ and $r_{\rm in} = 3.0^{+0.3}_{-0.4}$. However, the significance of detection of relativistic smearing is reduced with respect to the reflection models which do not include Comptonization of the line and edge features. The PEXRIV-based reflection models give $\Delta\chi^2 \sim 190$ for removing all smearing from the model, while the CDID reflection models give $\Delta\chi^2 \sim 13$.

Figs 2(b) and (c) show these fits with extreme relativistic smearing, and no relativistic smearing, respectively. It is clear that the *intrinsic* reflected emission alone – mainly the edge in the reflected continuum rather than the line itself, as there is very little line emission at these high ionizations – can match most of the broad feature in the data. This can have a strong impact on the detection significance of relativistic smearing and some impact on the detailed parameters. Plainly, it is important to use an accurate description of ionized reflection. However, there is considerable uncertainty in these models as they depend on the (unknown) vertical and radial ionization structure of the disc. The CDID models assume that the reflecting material can be approximated by a slab of constant (vertical and radial) density. Yet, a disc is in hydrostatic equilibrium so its structure *responds* to the incident radiation (Nayakshin, Kazanas & Kallman 2000; Ballantyne, Ross & Fabian 2001b). The upper layers are heated to the Compton temperature of the illuminating flux, so they expand, becoming less dense and more ionized. For hard power-law illumination the Compton temperature is large, so the upper layers are completely ionized, forming a skin on top of the disc, but for softer illuminating spectra (such as that of the data used here) the upper layers of the disc are still visible so the difference between the hydrostatic and constant ionization reflection models is much smaller (Done & Nayakshin 2001). As well as this vertical structure, there should also be a *radial* dependence of the ionization structure of the disc, and the full reflected emission should be the emissivity-weighted integral of all of these different-radii regions with vertical ionization structure.

We use the XION code (Nayakshin et al. 2000) to model reflection from a *disc* of material in hydrostatic equilibrium from power-law illumination, i.e. including both radial and vertical ionization gradients. This can be used to produce the total emission (direct plus reflected), in which the contribution of reflection is hardwired into the spectrum for a given geometry. However, in order to give a comparable number of degrees of freedom as in the CDID fits, we use XION to calculate the reflected emission *only*, and add a power law as the incident continuum so that the fraction $\Omega/2\pi$ is allowed to vary. We use the magnetic flares geometry to calculate the reflected emission from 10 to 100 Schwarzschild radii from a disc accreting at $L/L_{\rm Edd} = 0.05$ (see Fig. 1). The XION code includes relativistic smearing, but only for non-rotating black holes, so we switch this off and use the CONLINE convolution model as before. This gives a somewhat worse fit than before, with $\chi^2/\nu = 100/67$. A better fit can be obtained by setting $L/L_{\rm Edd} = 1$, with $\chi^2/\nu = 86.1/67$. This is due to the higher disc density expected at higher mass accretion rates. Both models give $r_{\rm in} \sim 2.2 \pm 0.2$ and $q \sim 3.5 \pm 0.3$ and again the best fit is reflection dominated.

### 4.3 Inclination

The inclination of the system is not well known, but recent studies of the companion star indicate that its *minimum* value is $50^\circ \pm 3^\circ$ (Orosz et al. 2004), showing that the assumption of 45° in the previous fits is probably too low.

The filled squares in Fig. 3(a) show the increase in $\chi^2$ with inclination for the fits for the CDID reflection models. Plainly, the lower inclination fits are preferred by the data. However, we note that there is no minimum in $\chi^2$ at 45° as seen from PEXRIV-based reflection models (Miller et al. 2002), so removing the only reason for using

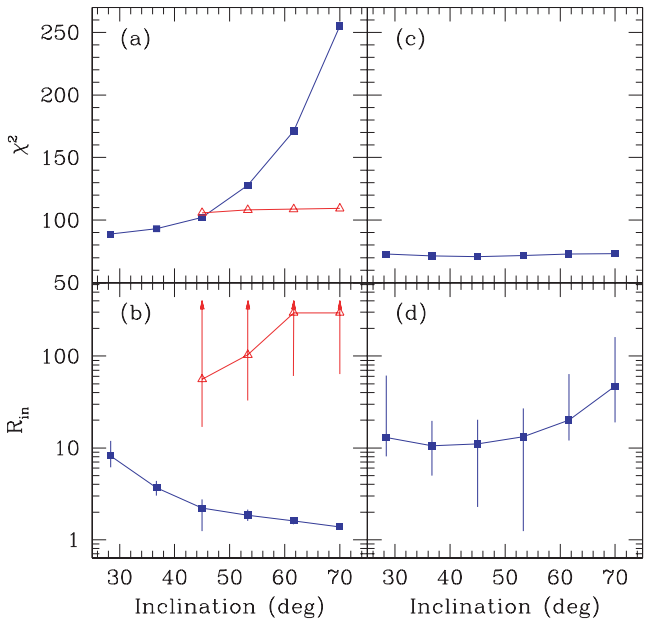


**Figure 3.** Panel (a) shows the inclination dependence of $\chi^2$ for the MECS data fit with a disc blackbody and relativistically smeared CDID ionized reflection with $q = 3$. The best-fitting solution switches between a highly smeared model (filled squares, blue in colour) and a mostly unsmeared solution (open triangles, red in colour). Panel (b) shows the derived disc inner radius for each solution. For the extreme smearing, the increase in inclination causes a large blueshift of the relativistic transfer function which is compensated by the fit by increasing the gravitational redshift, i.e. decreasing the inner radius. However, this also leads to increased broadening of the spectral features, and the total spectral shape does not match the data as well as at lower inclinations. Conversely, for the mostly unsmeared fit, there is very little change with inclination in either $\chi^2$ or derived radius. Panels (c) and (d) show how these results change with the inclusion of outflowing ionized absorption (predominantly blueshifted H- and He-like iron resonance lines). This gives better fits at *all* inclinations, for a disc inner radius which is always consistent with being larger than $6R_g$.

this inclination. These fits become very unstable so we fix $q = 3$ and assume that the continuum is purely reflected emission (i.e. no intrinsic continuum visible) in order to produce the plots. However, we checked that these assumptions do not qualitatively affect the results, unless we allow for extremely centrally concentrated emission. We can obtain good fits with $\chi^2 \sim 92$ at higher inclinations up to 70°, but only with $q \sim 15$.

At higher inclinations, the highly smeared solution becomes a worse fit to the data because of the increasing blueshift of the relativistic transfer function due to the larger projected line of sight velocities (e.g. Fabian et al. 1989). The fit compensates for this by increasing the gravitational redshift, i.e. by decreasing the disc inner radius and/or by increasing $q$. Since this figure is made for constant $q = 3$ then this requires that the inner radius decreases. However, this does not give enough gravitational redshift to compensate for the increased line broadening and most of the increase in $\chi^2$ comes from this increased blue extent of the spectral features. These extremely smeared fits then have a *worse* $\chi^2$ than the very different fits in which the line is mostly *unsmeared*, as described in Section 4.2 (see Fig. 2c). This solution is mostly independent of inclination as the intrinsic shape of the reflected emission below 10 keV is independent of inclination (Magdziarz & Zdziarski 1995), as are the relativistic effects for large inner disc radii. Because these two solutions, the extremely smeared and almost unsmeared, are far apart in parameter space, they give a double minimum in $\chi^2$ space. We show the $\chi^2$ for the mostly unsmeared fits as the open triangles in Fig. 3(a), and it is plain that these are a much better description of the data for inclinations above 45° than the highly smeared fits (filled squares). Fig. 3(b) shows the corresponding disc inner radius inferred for each solution as a function of inclination. Plainly, as the best fit switches between these two very different solutions, there is a corresponding dramatic jump in inferred disc inner radius.

The residuals to the (mostly) unsmeared fit for an inclination of 45° in Fig. 2(c) show a clear feature at ∼7.5 keV [the smeared fit in Fig. 2(b) also shows a similar feature]. This looks like a fairly narrow absorption feature, and including a narrow, Gaussian line (with best-fitting energy 7.58 keV and equivalent width of ∼100 eV) improves the fit by $\Delta\chi^2 = 17.4$, making it *significantly better*. The relativistic smearing reduces *dramatically*, now being entirely consistent with $q = 3$, and with a larger disc inner radius, $r_{\rm in} = 9^{+11}_{-4}$.

### 4.4 Narrow resonance line absorption

Motivated by the fits above, we consider how such absorption lines can occur. Observationally, strong resonance absorption lines are often seen from high-inclination Galactic binary systems, generally from iron K$\alpha$ He- and H-like iron at 6.7 and 7.0 keV (e.g. Ueda et al. 1998; Kotani et al. 2000; Lee et al. 2002; Ueda et al. 2004). However, if this absorbing material is outflowing then substantial blueshifts could be observed, and are seen in AGNs (Pounds et al. 2003). If the feature at ∼ 7.6 keV is an absorption line from iron then this implies a velocity of ∼0.09$c$ or 0.13$c$ depending on whether the identification is with the H- or He-like ion.

We use the XSTAR photoionization models which are publicly available as XSPEC multiplicative model tables. We choose the ones calculated for power-law illumination of a constant-density photoionized column with turbulent velocity of 100 km s$^{-1}$. This gives an improved $\chi^2$ for *all* inclinations with the CDID reflection models [see Fig. 3(c)], and dramatically changes the inferred smearing of the reflected emission [Fig. 3(d)]. The relativistic line is now *always* consistent with the illumination of $q = 3$ expected from gravitational energy release, and the inner disc radius is greater than $6R_g$.

The existence of several narrow features in the ionized absorber between 6.6 and 7 keV means that $\chi^2$ space is complex, with multiple local minima. However, the column in all fits is $\sim 10^{22}$ cm$^{-2}$ of ionized material ($\xi \sim 100$ erg cm s$^{-1}$) outflowing at ∼0.1–0.15$c$, with the best-fitting redshift of $0.151^{+0.007}_{-0.003}$. This model for an inclination of 45° is shown in Fig. 2(d).

This effect is only seen when using the newer models of reflection from ionized material, which include the self-consistent Comptonization of the iron line and edge by the hot upper layers of the disc. Fig. 4 (grey or green in colour, line) shows the best-fitting model using the PEXRIV-reflected continuum and narrow Gaussian line, convolved with the LAOR relativistic profile. The sharp drop at ∼7.2 keV seen in the data can be matched by the sharp blue wing of the relativistically smeared, intrinsically *narrow* line. By contrast, the black line in Fig. 4 shows the best-fitting model using the extremely smeared, highly ionized CDID reflection. The upper layer of the irradiated reflecting material is hot, so Comptonizes much of the line and edge, blending them together and making an intrinsically rather smooth spectrum (Ross et al. 1999). Convolution of this spectrum with relativistic effects makes it even broader, so there is no sharp change in curvature produced by the blue wing of the line. Since the data does have a sharp drop at 7.2–7.8 keV, these more physically self-consistent models of reflection give a worse fit. The

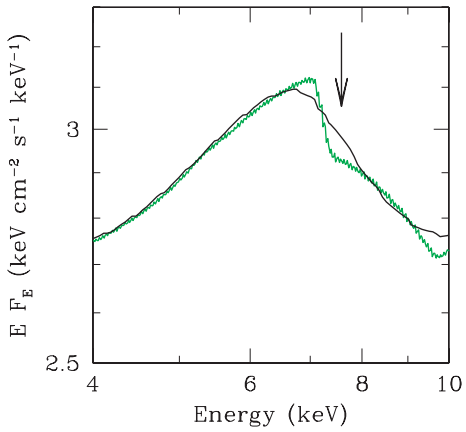


**Figure 4.** The grey (green in colour) line shows the best-fitting extreme smearing model where the intrinsic reflected emission is described by PEXRIV and a narrow Gaussian line (Section 4.1). The sharp edge to the transfer function gives the steep drop of the blue wing of the iron line, while the deep edge in the ionized reflected continuum is smoothed into a broad feature. There is a fairly steep drop in the data at 7.2 keV so this model can match the curvature seen (see Fig. 2). The black line shows the best-fitting extremely smeared CDID model (Section 4.2). The line and edge are now mostly blended together, intrinsically broadened by Comptonization in the intensely irradiated, hot upper layers of the reflecting slab. Relativistic broadening further smoothes the spectrum, so there is no sharp drop at 7.5 keV. Since this drop is present in the data, this model is a worse fit despite it being physically more realistic. The arrow shows the energy inferred when fitting an additional absorption line to the data.

significant residuals in the spectrum at ∼7.5 keV then are better fit by including outflowing absorption, predominantly resonance iron K lines at rest-frame energies of 6.7 and 6.95 keV. The drop seen in the data then no longer drives the relativistic line profile to extreme parameters and the derived smearing is completely compatible with a truncated disc.

### 4.5 Summary of MECS fits

There is a clear broad residual associated with iron in these *BeppoSAX* data from XTE J1650−500. Simple models of reflection, which ignore Comptonization of the line, require that the relativistic effects are extreme, implying a spinning black hole and perhaps direct extraction of the spin energy. However, these models also require that the reflected emission is highly ionized. This means that Comptonization of the line and edge is important, making these features *intrinsically* broad and blended together. The strength and significance of relativistic effects are then determined by the detailed modelling of the intrinsic reflected emission, which in turn depends on the (poorly known) vertical and radial structure of the disc. Nevertheless, the current best models of ionized reflection always pick out parameters where the innermost radius of the emitting material is much closer than $6R_g$, and with radial emissivity rather steeper than that expected from gravitational energy release alone. However, the smearing derived from these (best available) reflection models are *not* robust to changes in inclination, nor to the addition of ionized absorption features. While either (or both) of these effects can resolve the discrepancy of the inner disc radius derived from the line shape with that inferred from the overall evolution of spectral and timing features, a further conflict remains which is that the fits favour a reflection-dominated solution.

## 5 MECS AND PDS 2–200 keV: COMPLEX CONTINUUM MODELS

### 5.1 Simple reflection models

To get more constraints on the amount of reflection requires data at higher energies, so we include the simultaneous PDS data to extend the spectrum up to 200 keV. However, the spectrum is now much more sensitive to details of the continuum modelling due to the wide bandpass, and it is obvious that a power law can no longer be used. Even an exponentially cut-off power law is not a good approximation to the shape of a thermally Comptonized spectrum over such a wide bandpass. The rollover at energies close to the electron temperature, $kT_e$, is rather sharper than an exponential (Gierliński et al. 1997). Also, there are indications that the spectra can be more complex than predicted by just a single temperature thermal Compton component, with signatures of both thermal and non-thermal electrons even in the low/hard state (McConnell et al. 2000; Ibragimov et al. 2005).

We use the EQPAIR continuum model (Coppi 1999) in order to model the curvature of the Comptonized continuum. This computes the Comptonization of seed photons by a steady-state electron distribution which is *calculated* self-consistently from balancing an initial heating rate with Compton and Coulomb cooling processes. The code allows the input heating to be either non-thermal, with electrons injected with a power-law distribution of $Q(\gamma) \propto \gamma^{-s}$, between Lorentz factors $\gamma_{\rm min}$ and $\gamma_{\rm max}$ or thermal or some combination of both. However, even if *all* the electron heating is non-thermal, the self-consistent electron distribution (and hence output Comptonized spectrum) can be mainly thermal with only a small non-thermal tail if Coulomb collisions dominate the electron cooling. This happens where the power injected in the hard electrons, $l_{\rm h}$ (parametrized as a compactness $l = L\sigma_T/Rm_ec^3$; see e.g. Coppi 1999) is larger than that injected in soft photons, $l_{\rm s}$. Conversely, where the soft photons dominate then Compton cooling is most important, and the electron distribution retains a mainly power-law shape with only a small thermal component (Poutanen & Coppi 1998).

As well as calculating the curvature of the Comptonized spectrum at high energies, EQPAIR also computes the low-energy cut-off due to the seed photon distribution. This cut-off is typically at a few $kT_{\rm seed}$, so is *within* the observed bandpass for the MECS data. This curvature can make a large difference to the inferred disc temperature and luminosity (see e.g. Done, Życki & Smith 2002), and could potentially distort the inferred spectrum in the red wing of the iron line. We assume that the seed photons are the same as the observed disc photons in all the fits below, and fix $l_{\rm s} = 10$.

This continuum complexity means that we cannot easily use the CDID reflection models since these are tabulated assuming a cut-off in the continuum at a fixed energy of 100 keV. The assumed high-energy continuum shape affects the reflected emission at energies above ∼15 keV due to the predominance of Compton downscattering. Instead, we use the reflection model in EQPAIR (which is based on PEXRIV but reflecting the self-consistent continuum from EQPAIR), together with a Gaussian line. We relativistically smear both reflected continuum and line with the LAOR kernel, now extending the bandpass for the convolution calculation from 0.2 to 1000 keV, and assume an inclination of 45°. Purely thermal electron heating gives an (almost) acceptable fit, with $\chi^2_\nu = 99.9/79$ for a reflection-dominated ($\Omega/2\pi = 2.4^{+1.5}_{-0.8}$), highly smeared fit ($q = 3.8 \pm 0.2$, $r_{\rm in} = 1.8^{+0.3}_{-0.1}$). However, purely non-thermal injection models give a significantly better fit, with $\chi^2 = 82.7/78$ (there is one extra free parameter which is the spectral index of the power-law electron injection). The subtle difference in

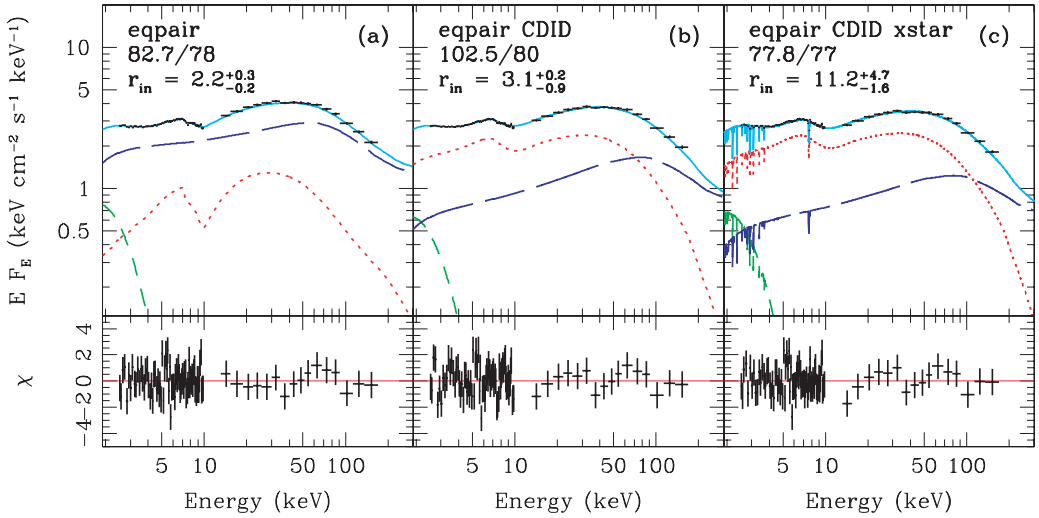


**Figure 5.** MECS and PDS data fit with a disc blackbody (dashed curve, green in colour) and EQPAIR continuum (long-dashed, blue in colour), together with the reflection (dotted, red in colour) from the disc. Panel (a) shows the model with simple reflection, panel (b) with CDID reflection and panel (c) the same, but with ionized blueshifted absorption added.

continuum curvature means that the solution is no longer reflection dominated, with $\Omega/2\pi = 0.72^{+0.12}_{-0.08}$ though it is still strongly smeared ($q = 3.5^{+0.3}_{-0.2}$ and $r_{\rm in} = 2.2^{+0.3}_{-0.2}$). The MECS and PDS spectrum and residuals for this best-fitting non-thermal injection model are shown in Fig. 5(a).

### 5.2 Complex reflection models

Section 4.2 showed that there are large differences in the model spectra for ionized reflection. While the CDID reflection models concentrate on the spectra below ∼12 keV, computing the effects of photoionization and Compton upscattering and downscattering at low energies, they do not accurately treat Compton scattering at higher energies, nor include angle-dependent effects, nor allow for different illuminating continua. This contrasts with the PEXRIV models of reflection which have very approximate ionization balance (Done et al. 1992) and neglect Comptonization below 12 keV, but treat Comptonization at higher energies very accurately, and give the reflected emission as a function of observed inclination angle. PEXRIV is based on the convolution kernels given by Magdziarz & Zdziarski (1995), so can be extended to work with *any* illuminating continuum.

Plainly, what is needed is a combination of these models, using the better CDID photoionization/Compton scattering of reflection at low energies and the PEXRIV accurate Compton downscattering at higher energies. The most flexible way to incorporate this is as a convolution model in XSPEC, so that the reflected spectrum can be calculated for any arbitrary continuum. We have coded this by finding the PEXRIV cross-section at 10 keV which gives the same 12–14 keV reflected spectrum gradient as the CDID models for a given ionization parameter and illuminating spectral index. The corresponding PEXRIV Green's functions are used to form the spectrum above 12 keV. Below 12 keV the Green's functions are assumed to collapse to delta functions, given by the ratio of reflected to incident flux in the CDID models, rescaled to match the normalization of PEXRIV at 14 keV. This model is hereafter called REFBAL.

We use this together with the EQPAIR continuum model, and get a somewhat worse fit than for the PEXRIV models, with $\chi^2 =$ 102.5/80 for an illuminating continuum from non-thermal injection. This is shown in Fig. 5(b) and by contrast with the PEXRIV reflection, it requires a larger fractional contribution from reflection, with $\Omega/2\pi = 2.0^{+1.2}_{-0.7}$. However, both PEXRIV- and CDID-based models require that reflection is highly smeared, with $r_{\rm in} = 2$–3.

We then include the narrow absorption features from XSTAR ionized absorption. As with the MECS data alone, this dramatically reduces the derived relativistic smearing to being consistent with a disc truncated *above* $r_{\rm in} = 6$ for the CDID reflection models. However, the fit still has $\Omega/2\pi = 2.4^{+0.5}_{-0.4}$, which is reflection dominated, although there is a significant contribution from the intrinsic continuum component as well.

### 5.3 Summary of MECS and PDS fits

The inclusion of the PDS data up to 200 keV plainly gives more constraints on the amount of reflection than the MECS data alone. With data only up to 10 keV the amount of reflection is very poorly defined, and the spectrum can be pure reflected emission with no intrinsic continuum. Including the higher-energy data shows that there is most probably true continuum present, though the derived reflected fraction is sensitive to details of how the reflected and continuum emission are modelled. With the PEXRIV-based reflection models, the data are consistent with $\Omega/2\pi < 1$ as expected for a truncated disc, while the more physical CDID-based reflection models have substantially more reflection present, with $\Omega/2\pi \sim 2$. Both these require extreme smearing and emissivity, but like the MECS-only fits, the smearing is again sensitive to the inclusion of narrow absorption lines from an ionized outflow for the CDID reflection models.

## 6 DISCUSSION

The bright low-/hard-state spectrum seen by *BeppoSAX* from the transient black hole XTE J1650−500 is certainly consistent with extremely smeared, reflection-dominated emission as claimed by Miniutti et al. (2004). However, it is also consistent with much less smearing if there is some ionized, outflowing absorption which gives narrow resonance lines at ∼7.5 keV. Reducing the amount of

smearing makes the reflected iron line consistent with the expectations of truncated disc models, removing the conflict between the position of the inner edge of the cool disc derived from the broad-band spectral shape and QPOs. This is *directly testable* with high-resolution data around the iron line.

Such absorbing material is *often* seen in X-ray binaries, especially those at fairly high inclination angles (Ueda et al. 1998; Kotani et al. 2000; Lee et al. 2002; Ueda et al. 2004), including XTE J1650−500 (Miller et al. 2004a). The one difference here is that the outflowing material has velocity $\sim 4.5 \times 10^4\,\mathrm{km\,s^{-1}}$, much higher than the $\sim$500 km s$^{-1}$ typically seen in these objects. A low-velocity wind would be launched from fairly large radii in the disc, as expected for line driving from the ultraviolet-emitting region of the GBH disc (Proga & Kallman 2002). By contrast, the much higher velocities required here would need to be associated with a launch from the inner accretion disc, where line driving is not effective due to the high ionization. This suggests rather that the wind would have to be magnetically driven, and/or be associated with the jet. We note that these data are taken shortly after the time of the maximum in radio emission (Corbel et al. 2004), so the inferred very fast outflow could be associated with the jet ejection.

We can estimate the mass-outflow rate. For a constant-velocity outflow the mass-outflow rate at a radius $R$ is

$$\dot{M}_{\rm out} = 4\pi R^2 n m_{\rm p} f v, \tag{1}$$

where $n$ is the number density of the outflowing material, $v$ is its velocity, $f \equiv \Omega/4\pi$ is the fractional solid angle in which the outflow is directed and $m_{\rm p}$ is the proton mass. In a steady state $\dot{M}_{\rm out}$ is constant for all radii. The column density measured by the observer is

$$N_H = \int_{R_{\rm in}}^{\infty} n\,{\rm d}R = \frac{1}{4\pi f m_{\rm p}} \frac{\dot{M}_{\rm out}}{R_{\rm in} v}, \tag{2}$$

therefore

$$\dot{M}_{\rm out} = 4\pi f m_{\rm p} N_H R_{\rm in} v. \tag{3}$$

For $N_H = 10^{22}\,\mathrm{cm^{-2}}$, $R_{\rm in} = 10R_g$, $v = 0.15c$ and $f \leqslant 1$ we find $\dot{M}_{\rm out} \lesssim 1.4 \times 10^{16}\,\mathrm{g\,s^{-1}} \approx 10^{-3}\dot{M}_{\rm Edd}$ (assuming accretion efficiency of 0.1 and black hole mass of $10\,\mathrm{M}_\odot$). This is only about 1 per cent or less of estimated inflow mass accretion rate and constitutes a very feasible number.

Our spectral fitting also shows that this absorption does *not* make the data consistent with all the expectations of a truncated disc. The best current models of reflection based on irradiation of a slab of constant density give reflection fractions which are much larger than expected for a truncated disc geometry. This is not necessarily the case using the older PEXRIV-reflection models, which can give much smaller reflection fractions. The difference is due to Comptonization of the line and edge in the reflected emission as it travels through the upper layers of the disc (Ross et al. 1999). This effect is neglected in PEXRIV, so the iron edge is rather sharp. On the other hand, the CDID reflection is not calculated for the disc temperatures appropriate for Galactic binaries, i.e. 0.5–1 keV. In such hot material, collisional processes alone will ionize iron up to the K shell (Davis et al. in preparation). By contrast, the CDID models do not include collisional ionization, and thus require intense illumination to ionize iron up to the K shell to match the data. This pulls the temperature of the upper layers to the Compton temperature of 1.5–2 keV, for spectra with $\Gamma \sim 1.9$–2 (Ross et al. 1999; Nayakshin et al. 2000). This is a factor of 2–3 larger than the observed disc temperature in these data. Thus, while the PEXRIV models underestimate the width of the line and edge by having no Compton scattering below 12 keV, the CDID models may overestimate it for Galactic binaries. From our spectral fits, the derived reflected fraction is sensitive to the detailed shape of this edge. Better models of reflection for conditions appropriate to Galactic binary discs will enable this effect to be quantified, removing this as a source of uncertainty.

The amount of reflection is also sensitive to the detailed form assumed for the continuum. This is not easily defined even with broad-bandpass data. Obviously, the wider the bandpass, the more constraints there are on the form of the continuum curvature, but also the more the spectrum is sensitive to the detailed form of continuum assumed. Broad-bandpass data suggest that the spectrum has convex curvature which can be modelled by an additional soft excess component (e.g. Di Salvo et al. 2001; Ibragimov et al. 2005). This makes the intrinsic continuum at higher energies rather harder than expected from the observed 2–10 keV emission, reducing the amount of reflection required to match the data at high energies. Including such a component in the model makes the reflected fraction almost completely undetermined and consistent with a truncated disc with the REFBAL and ionized absorber models. Such additional continuum complexity is not required statistically from the spectral data alone (even with the moderate spectral resolution and broad bandpass of *BeppoSAX*). However, energy-resolved *variability* could give additional constraints as such data can fairly unambiguously pinpoint the seed photon energy seen by the Comptonizing plasma (Gierliński & Zdziarski 2005), so could disentangle the shape of the soft emission.

## 7 OTHER EXTREME LINE OBJECTS

Most detections of extreme broad iron lines in GBH are in the very high state (alternatively named the steep power-law state) rather than in the low/hard state examined here (see e.g. Miller et al. 2004a). This (typically rather high mass accretion rate) spectral state shows strong disc emission as well as a strong, steep high-energy tail, while the power spectrum of the variability shows a strong QPO which is close to its maximum frequency (e.g. McClintock & Remillard in press). Thus, both spectral and timing properties imply that the inner disc does extend close to the black hole [quite how close is difficult to determine due to the complexity of the spectra: Kubota & Done (2004), Done & Kubota (2006)]. Thus there are no obvious conflicts as for the low/hard state. There are objects where the disc-dominated spectra imply moderate spin (from the $L_{\rm disc} \propto T_{\rm max}^4$ relation) while the iron line smearing implies extreme spin but these could be explained by the accretion flow extending below $R_{\rm ms}$ in the very high state (Reynolds & Begelman 1997).

However, there *is* a more subtle conflict with the extreme line in these data which is that the very high-state spectra typically show strongly Comptonized emission. The broad-band spectral shape seen in, for example, the simultaneous *ASCA–RXTE*–OSSE data from XTE J1550−564 implies that the inner disc is almost completely covered by material with optical depth 2–3 (Done & Kubota in preparation; Gierliński & Done 2003). Thus, the spectral shape implies that very little of the inner disc is seen directly, so it *cannot* make much contribution to the line emission. Yet the *same ASCA* data require an extreme broad line when fit by PEXRIV-based models (Miller et al. 2004b). Again, we suggest that resonance line absorption in an outflowing wind can modify the derived line width and remove these conflicts in the very high-state spectra. To test this, we fit the publicly available standard products gas imaging spectrometer data, as this does not suffer from the pileup problems of the solid-state imaging spectrometer for such a bright source. The relativistic smearing required for a PEXRIV-reflected continuum and narrow line are extreme, with $r_{\rm in} = 1.6^{+0.3}_{-0.4}$ and $q = 3.7 \pm 0.3$, with

$\chi^2 = 796.5/742$, similar to the parameters found by Miller et al. (2004b). Replacing this with CDID reflection gives similar extreme relativistic smearing but a worse fit ($\chi^2 = 824.6/744$). Including XSTAR ionized absorption improves the fit ($\chi^2 = 805.4/741$), and as in XTE J1650−500 this reduces the relativistic effects to the point where $r_{\rm in} = 31_{-15}$ (no upper limit) with $q$ fixed at 3.

The *extreme* broad lines inferred in some AGNs are similarly potentially affected by absorption complexity changing the line parameters. Here, there are as yet no obvious problems with this interpretation, especially as extreme spin might be *expected* given the hierarchical growth of black holes through accretion (Volonteri et al. 2005). None the less, if the apparently extreme GBH iron lines are actually consistent with low spin, normal illumination rather than extraction of rotational energy from an extreme spin black hole, then it is likely that the AGN discs behave similarly. We note that the recent *Chandra* spectrum of the most secure extreme relativistic line, that in MCG–6-30-15, reveals the presence of ionized absorption at a similar column and ionization as that required here to reduce the relativistic smearing to levels consistent with a truncated disc (Young et al. 2005). Young et al. (2005) checked that this absorption did not change the extreme smearing deduced from a LAOR description of the line, but this is unsurprising due to the unphysically sharp blue wing of the line produced in such models (see Fig. 4). Our fitting showed that the relativistic line parameters only changed significantly when using the CDID highly ionized reflection models as these have a much smoother intrinsic spectrum around the iron line/edge due to Comptonization. We urge testing the robustness of the extreme relativistic effects to the inclusion of ionized absorption with more physical ionized reflection models.

## 8 CONCLUSIONS

The truncated disc/hot inner flow geometry is very successful in qualitatively (and sometimes quantitatively) explaining many disparate properties of the low/hard state in GHB. If the radius at which the hot flow evaporates from cool disc progressively decreases as the source approaches the transition to the soft state, then this can account for the observed evolution in spectral and timing properties. However, if there really are detections of substantial amounts of iron line emission from cool disc-like material down at the last stable orbit *in the low/hard state*, then the truncated disc idea is simply wrong. Some of the extreme line emission might be explained by clumps from a disrupted disc embedded in the hot flow, but this would give rise to only a small amount of line since the covering fraction of the clumps would be rather less than that from a disc, and these are embedded in a hot flow with optical depth of around unity, so Compton scattering suppresses the line.

We show that the bright low-/hard-state spectrum seen by *BeppoSAX* from the transient black hole XTE J1650−500 can indeed be interpreted as requiring strong, extremely smeared reflected emission from a disc-like structure extending down to $\sim 2R_g$ as shown by Miniutti et al. (2004). These data clearly illustrate the conflict between this and the position of the inner edge of the cool disc derived from the broad-band spectral shape and QPOs. The small inner radius inferred from the line width also conflicts (though more weakly) with the moderate spin inferred both from theoretical models of stellar collapse and from the observed $L_{\rm disc} \propto T_{\rm max}^4$ relation in this object. We show that *all* these conflicts can be removed if relativistic effects on the line and reflected continuum are overestimated due to the presence of absorption line features in the spectrum. The derived line width is then easily found to be consistent with normal emissivity and a disc truncated at $\sim$10–20$R_g$ (so giving no information on the black hole spin). The reflection feature are most probably shaped by strong, but not necessarily extreme, gravity. We suggest that this effect is robust, i.e. that moderate columns of highly ionized absorbing material (predominantly resonance lines of H- and He-like iron) can *always* reduce the inferred relativistic smearing of a highly ionized reflected spectrum. This could then remove the more subtle conflict seen in the very high-state GBH spectra, where the disc should be down close to the last stable orbit (so strong relativistic smearing is expected) but the spectral shape shows that the inner disc is mostly covered by an optically thick, hot corona. We stress that the presence of absorption at this level is directly *testable* with high-resolution data.

While there are no such direct conflicts for AGNs, we note that the most secure extreme line candidate, MCG–6-30-15, has highly ionized reflection (e.g. Wilms et al. 2001) and a recent *Chandra* High-Energy Transmission Grating spectrum shows absorption at the same column and ionization (Young et al. 2005) as inferred here for XTE J1650−500. We urge a re-analysis of these data to see whether the extreme line parameters are robust to the presence of absorption when using the more physical reflection models which include self-consistent Comptonization of the line and edge as opposed to models in which the line is intrinsically narrow.

## ACKNOWLEDGMENTS

MG and CD thank PPARC for support through a fellowship and senior fellowship, respectively.

## REFERENCES

Abramowicz M. A., Igumenshchev I. V., 2001, ApJ, 554, L53
Arnaud K. A., 1996, in Jacoby G. H., Barnes J., eds, ASP Conf. Ser. Vol. 101, Astronomical Data Analysis Software and Systems V. Astron. Soc. Pac., San Francisco, p. 17
Ballantyne D. R., Iwasawa K., Fabian, 2001a, MNRAS, 323, 506
Ballantyne D. R., Ross R. R., Fabian A. C., 2001b, MNRAS, 327, 10
Barrio F. E., Done C., Nayakshin S., 2003, MNRAS, 342, 557
Balbus S. A., Hawley J., 1991, ApJ, 376, 214
Beloborodov A. M., 1999, ApJ, 510, L123
Blandford R. D., Begelman M. C., 1999, MNRAS, 303, L1
Churazov E., Gilfanov M., Revnivtsev M., 2000, in SGSC Conf. Ser. Vol. 1, Proc. 5th Sino–German Workshop on Astrophysics. China Science & Technology Press, Beijing, p. 114 (astro-ph/0002415)
Coppi P. S., 1999, in ASP Conf. Ser. Vol. 161. Astron. Soc. Pac., San Francisco, p. 375
Corbel S., Fender R. P., Tomsick J. A., Tzioumis A. K., Tingay S., 2004, ApJ, 617, 1272
Cui W., Zhang S. N., Chen W., Morgan E. H., 1999, ApJ, 512, L43
Di Salvo T., Done C., Życki P. T., Burderi L., Robba N. R., 2001, ApJ, 547, 1024
Done C., 2001, Adv. Space Res., 28, 255
Done C., Gierliński M., 2003, MNRAS, 342, 1041
Done C., Kubota A., 2006, MNRAS, submitted (astro-ph/051130)
Done C., Nayakshin S., 2001, ApJ, 546, 419
Done C., Mulchaey J. S., Mushotzky R. F., Arnaud K. A., 1992, ApJ, 395, 275
Done C., Życki P., Smith D. A., 2002, MNRAS, 331, 453
Ebisawa K., Makino F., Mitsuda K., Belloni T., Cowley A. P., Schmidtke P. C., Treves A., 1993, ApJ, 403, 684
Esin A. A., McClintock J. E., Narayan R., 1997, ApJ, 489, 865
Esin A. A., McClintock J. E., Drake J. J., Garcia M. R., Haswell C. A., Hynes R. I., Muno M. P., 2001, ApJ, 555, 483
Fabian A. C., Rees M. J., Stella L., White N. E., 1989, MNRAS, 238, 729

Fabian A. C., Iwasawa K., Reynolds C. S., Young A. J., 2000, PASP, 112, 1145
Falcke H., Körding E., Markoff S., 2004, A&A, 414, 895
Frontera F. et al., 2001, ApJ, 561, 1006
Gammie C. F., Shapiro S. L., McKinney J. C., 2004, ApJ, 602, 312
Gierliński M., Done C., 2003, MNRAS, 342, 1083
Gierliński M., Done C., 2004, MNRAS, 347, 885
Gierliński M., Zdziarski A. A., 2005, MNRAS, 363, 1349
Gierliński M., Zdziarski A. A., Done C., Johnson W. N., Ebisawa K., Ueda Y., Haardt F., Phlips B. F., 1997, MNRAS, 288, 958
Hawley J. F., Balbus S. A., 2002, ApJ, 573, 736
Ibragimov A., Poutanen J., Gilfanov M., Zdziarski A. A., Shrader C. R., 2005, MNRAS, 362, 1435
King A. R., Kolb U., 1999, MNRAS, 305, 654
Kotani T., Ebisawa K., Dotani T., Inoue H., Nagase F., Tanaka Y., Ueda Y., 2000, ApJ, 539, 413
Kubota A., Done C., 2004, MNRAS, 353, 980
Kubota A., Makishima K., 2004, ApJ, 601, 428
Kubota A., Makishima K., Ebisawa K., 2001, ApJ, 560, L147
Lee J. C., Reynolds C. S., Remillard R., Schulz N. S., Blackman E. G., Fabian A. C., 2002, ApJ, 567, 1102
Li L.-X., Zimmerman E. R., Narayan R., McClintock J. E., 2005, ApJS, 157, 335
Lubiński P., Zdziarski A. A., 2001, MNRAS, 323, L37
Magdziarz P., Zdziarski A., 1995, MNRAS, 273, 837
McClintock J. E., Remillard R. A., in Lewin W. H. G., van der Klis M., eds, Compact Stellar X-ray Sources. Cambridge Univ. Press, Cambridge, in press
McConnell M. L. et al., 2000, ApJ, 543, 928
Miller J. M. et al., 2002, ApJ, 570, L69
Miller J. M. et al., 2004a, ApJ, 601, 450
Miller J. M., Fabian A. C., Nowak M. A., Lewin W. H. G., 2004b, in Proc. 10th Annual Marcel Grossmann Meeting on General Relativity, in press, preprint (astro-ph/0402101)
Miniutti G., Fabian A. C., Miller J. M., 2004, MNRAS, 351, 466
Narayan R., Yi I., 1995, ApJ, 452, 710
Nayakshin S., Kazanas D., Kallman T. R., 2000, ApJ, 537, 833
Orosz J. A., McClintock J. E., Remillard R. A., Corbel S., 2004, ApJ, 616, 376
Pounds K. A., Reeves J. N., King A. R., Page K. L., O'Brien P. T., Turner M. J. L., 2003, MNRAS, 345, 705
Poutanen J., Coppi P. S., 1998, Phys. Scr., T77, 57 (astro-ph/9711316)
Proga D., Kallman T. R., 2002, ApJ, 565, 455
Psaltis D., Norman C., 2000, preprint (astro-ph/0001391)
Reynolds C. S., Begelman M. C., 1997, ApJ, 488, 109
Ross R. R., Fabian A. C., 1993, MNRAS, 261, 74
Ross R. R., Fabian A. C., Young A. J., 1999, 306, 461
Rossi S., Homan J., Miller J. M., Belloni T., 2004, Nucl. Phys. B Proc. Suppl., 132, 416
Różańska A., Czerny B., 2000, MNRAS, 316, 473
Shafee R., McClintock J. E., Narayan R., Davis S. W., Li L.-X., Remillard R. A. 2005, ApJ, submitted, preprint (astro-ph/0508302)
Shakura N. I., Sunyaev R. A., 1973, A&A, 24, 337
Shapiro S. L., Lightman A. P., Eardley D. M., 1976, ApJ, 204, 187
Stella L., Vietri M., 1998, ApJ, 492, L59
Titarchuk L., Osherovich V., Kuznetsov S., 1999, ApJ, 525, L129
Tomsick J. A., Kalemci E., Corbel S., Kaaret P., 2003, ApJ, 592, 1100
Ueda Y., Inoue H., Tanaka Y., Ebisawa K., Nagase F., Kotani T., Gehrels N., 1998, ApJ, 492, 782
Ueda Y., Murakami H., Yamaoka K., Dotani T., Ebisawa K., 2004, ApJ, 609, 325
Volonteri M., Madau P., Quataert E., Rees M. J., 2005, ApJ, 620, 69
Wijnands R., van der Klis M., 1999, ApJ, 514, 939
Wilms J., Reynolds C. S., Begelman M. C., Reeves J., Molendi S., Staubert R., Kendziorra E., 2001, MNRAS, 328, L27
Young A. J., Lee J. C., Fabian A. C., Reynolds C. S., Gibson R. R., Canizares C. R., 2005, ApJ, 631, 733
Zdziarski A. A., Gierliński M., 2004, Prog. Theor. Phys. Suppl., 155, 99
Życki P. T., Done C., Smith D. A., 1998, ApJ, 496, L25

This paper has been typeset from a TEX/LATEX file prepared by the author.